

## **CHARACTERIZING VARIOUS ZONES FORMED IN FRICTION STIR SPOT WELDING WITH DIFFERENT TOOL PINS**

\*Ashu Garg and Anirban Bhattacharya

*Mechanical Engineering Department,  
Indian Institute of Technology Patna, Bihar, India  
(\*Corresponding author: ashu.pme16@iitp.ac.in)*

### **ABSTRACT**

Friction stir spot welding of aluminum alloy AA6061-T6 sheets was performed with circular (plunge depths 0.4 and 0.6 mm), square and triangular tool pin (plunge depth 0.4 mm) with constant 0.2 mm shoulder penetration to characterize various zones of weld nugget. It was observed that the depth of the stir zone formed below the tool pin is comparatively similar for different tool pins but wider for circular tool pin. The size of another stir zone formed at the interface of tool pin and a tool shoulder is observed to be larger for triangular and square tool pin due to the higher swept rate. Predicted strain from finite element analysis, calculated strain rate using Zener-Hollomon relationship and experimentally measured grain size distribution indicates severe amount of plastic deformation in-and-around the nugget/spot region. Finer grains in various stir zones were observed than thermo-mechanically and heat affected zones. Grain size (at distribution peaks) in stir zones varied around 2.54  $\mu\text{m}$  to 3.69  $\mu\text{m}$  for different tool pin profiles as compared to base metal grain size of 20  $\mu\text{m}$ . Microhardness results indicate that the welded region is quite softened than base metal and maximum hardness is mostly observed around the thermo-mechanically affected zone.

### **KEYWORDS**

Friction stir spot welding, Grain size, Hardness, Strain, Strain rate, Tool pin profile

## INTRODUCTION

Friction stir spot welding (FSSW) is widely used for joining the sheets of materials like aluminum, copper, magnesium, etc. The process begins by plunging a rotating tool (generally having a pin and a shoulder) into the sheets to be welded. Continuous stirring of the tool and downward plunging force generates localized heat due to friction at the tool-sheet interface and plastic deformation of the sheet metal. The material gets softened and the plasticized material adjacent to the tool pin starts flowing due to the action of tool rotation and tool plunge thereby causing intermixing and bonding between the overlapped sheets. The tool stirring also promotes grain refinement in the weld nugget associated with high strain, strain rate and thermal cycle. The formation of new microstructure also affects the mechanical properties and efficiency of FSSW joints. Studies also showed that the tool pin design and tool shoulder feature exerts a noteworthy influence on the material flow and intermixing during the FSSW process (Reilly et al., 2015; Hirasawa et al., 2010). Sarkar et al. (2016) studied the material flow and intermixing during FSSW using tracer material method and reported that the size and width of flow zone increases with tool penetration depth. The influence of tool rotational speed on microstructure and stir zone temperature was investigated during FSSW of dissimilar AA6061-AA5754 alloys (Gerlich et al., 2007). They reported that the average grain size in stir zone of AA6061 weld increases with increase in tool rotational speed. In another work, Gerlich et al. (2008) studied the local melting and tool slippage during FSSW of Al alloys. Tool slippage was investigated by calculating the strain rate using Zener-Hollomon relation. Garg and Bhattacharya (2017a) studied the effect of dwell time, tool pin profiles and tool rotational speed on shear strength, microstructure, temperature and strain distribution during FSSW of AA6061. In another work, Garg and Bhattacharya (2017b) analyzed the effect of different tool pins and pinless tools on the shear strength and microstructure during similar and dissimilar FSSW of AA6061-T6 and pure Cu. Chang et al. (2004) proposed mathematical relationship between the average grain size and Zener-Hollomon parameter during friction stir processing of Mg alloy. Solhjoon (2010) presented a mathematical approach to determine the critical strain as a function of peak strain required for initiation of dynamic recrystallization in austenitic stainless steel. Fratini and Buffa (2005) also proposed the numerical model to determine the grain size during continuous dynamic recrystallization phenomenon.

Aforesaid literature reveals that the different process parameters and tool pin shapes do significantly affect the thermal and material flow behavior during the FSSW process. The variation in failure modes and the strength of the FSSW joints might be attributed to the material flow and intermixing between the sheets to be welded and subsequent formation of various zones. Therefore, the formation of different zones, flow, intermixing and bonding between the sheets (joint strength) can significantly be dependent on the tool pin geometries in addition to the process parameters. In the present paper, detailed characterization of various zones of FSSW joints prepared with tools having different pin profiles (circular, square and triangular) and plunge depths (0.4 mm and 0.6 mm) are carried out through experimental investigations and finite element (FE) analysis.

## MATERIALS AND METHODS

In the present work, AA6061-T6 sheet (thickness 0.5 mm) was used as the workpiece material. The sheets were cut to dimensions of 105 mm  $\times$  45 mm and placed in lap configuration with 35 mm overlap for FSSW at the center of overlapped region. Tool rotational speed of 2500 rpm, downward plunge rate of 0.25 mm/min and dwell time of 4 s were kept constant. All tools were fabricated from H13 hot die steel. Tools were designed with circular tool pin with a shoulder of diameter 10 mm and pin diameter of 4.95 mm with two different pin lengths ( $l$ ) of 0.2 mm and 0.4 mm. Therefore, with a tool shoulder penetration of 0.2 mm, the total plunge depth ( $h_p$ ) attained as 0.4 and 0.6 mm, respectively. For square and triangular tools the shoulder diameter of 10 mm remains the same and the dimensions of pins were chosen such that the volume swept by the tool during rotation remains constant. Both triangular and square tools were made with pin length ( $l$ ) of 0.2 mm and constant shoulder penetration of 0.2 mm (thus  $h_p = 0.4$  mm) was imposed during FSSW. The detailed dimensions of FSSW tools are shown in Figure 1. The optical measuring microscope was used for metallographic examination of different zones of the welded joints. The micro-indentation was carried out to measure the micro-hardness at various zones of welded joints.

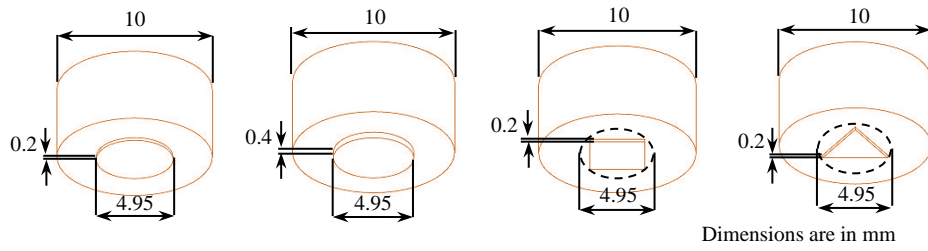


Figure 1. Schematic diagram of FSSW tools with different tool pin geometries

Finite element modeling and simulations were performed by creating a model only for an overlap region with a combined sheet thickness of 1 mm. The model was meshed by tetrahedron elements and finer mesh size was selected for the welded region. The different boundary conditions applied in the present FE model includes: sheet periphery fixed i.e. motion constrained in all three axis, upper and lower sheet surfaces are open to atmosphere for convection ( $h = 20 \text{ W/m}^2\text{-}^\circ\text{C}$ ) with ambient temperature  $20 \text{ }^\circ\text{C}$ , the tool rotation speed of 2500 rpm with downward plunging rate ( $-Z$  direction) of 0.25 mm/min and friction coefficient  $\mu = 0.2$ . The FSSW tool was modeled as rigid whereas the material properties of AA6061-T6 were taken from the software material library.

## RESULTS AND DISCUSSION

### Circular Tool Pin

Figure 2(a) shows the microscopic views of different zones formed below the tool surface for the FSSW joint prepared with circular tool pin and total penetration ( $h_p$ ) of 0.4 mm. Under the action of tool rotation, generated friction and plunge force the plasticized material beneath the tool pin surface starts flowing in downward direction followed by sidewise and outward movement. Furthermore, as the tool is plunged into the workpiece, the plasticized material from both upper as well as lower sheets start flowing together around the tool pin circumference and tool pin bottom due to friction at the tool-workpiece interface and forms a distinct stir region (Stir Zone-I, hereinafter denoted by SZ-I). The formation of SZ-I begins during the initial phase when the tool pin touches the upper metal sheet and gradually propagates along the thickness direction with the downward tool movement. The SZ-I is observed to be around 4.61 mm wide with maximum depth of 0.57 mm in this region (nugget cross sectional view, Figure 2(a)). As plunging progress and tool shoulder touches the upper sheet, the plastic flow of material spreads over a wider area (adds surface below the tool shoulder). The plasticized material below the shoulder gets extruded downward however the material closer to the pin periphery gets obstructed by the remaining solid material present outside the nugget thus flows back towards the pin center. Conversely, the material very close to the shoulder periphery manages to escape out through the shoulder circumference and forms a flash. The pin provides the outward spinning motion and pushed the material back below the tool shoulder region. This combination of two patterns results in a swirl flow pattern of plasticized material in the stir region (Stir Zone-II, SZ-II) around the intersection of tool pin and shoulder (Figure 2(a)). The maximum width and depth of SZ-II are measured around 0.95 mm and 0.59 mm, respectively and observed similar on both sides as can be seen from the sectional view (Figure 2(a)). Thus, the material flow during FSSW process is observed to happen possibly into two categories—the thickness flow in the vertical direction which forms the SZ-I and rotational flow around the tool pin periphery that leads to the formation of SZ-II. Another stir zone (Stir Zone III, SZ-III) is formed below the tool shoulder towards the periphery of shoulder due to friction at the tool shoulder bottom-workpiece interface and outward flow of plasticized material near the shoulder periphery. The microstructure of all stir zones (SZ) is characterized by finer equiaxed grain imposed due to dynamic recrystallization associated with high strain, strain rate and friction induced thermal cycle. Figure 2(a) (Region (1) and (3)) also shows the grain refinement adjacent to SZ which is known as thermo-mechanically affected zone (TMAZ) characterized by the highly deformed and finer grains associated with moderate strain rate and thermal cycle. Region (2) and (3) shows the grain

refinement adjacent to TMAZ commonly known as heat affected zone (HAZ) also characterized by the finer grains as compared to base metal (BM) due to exposure to the welding heat only.

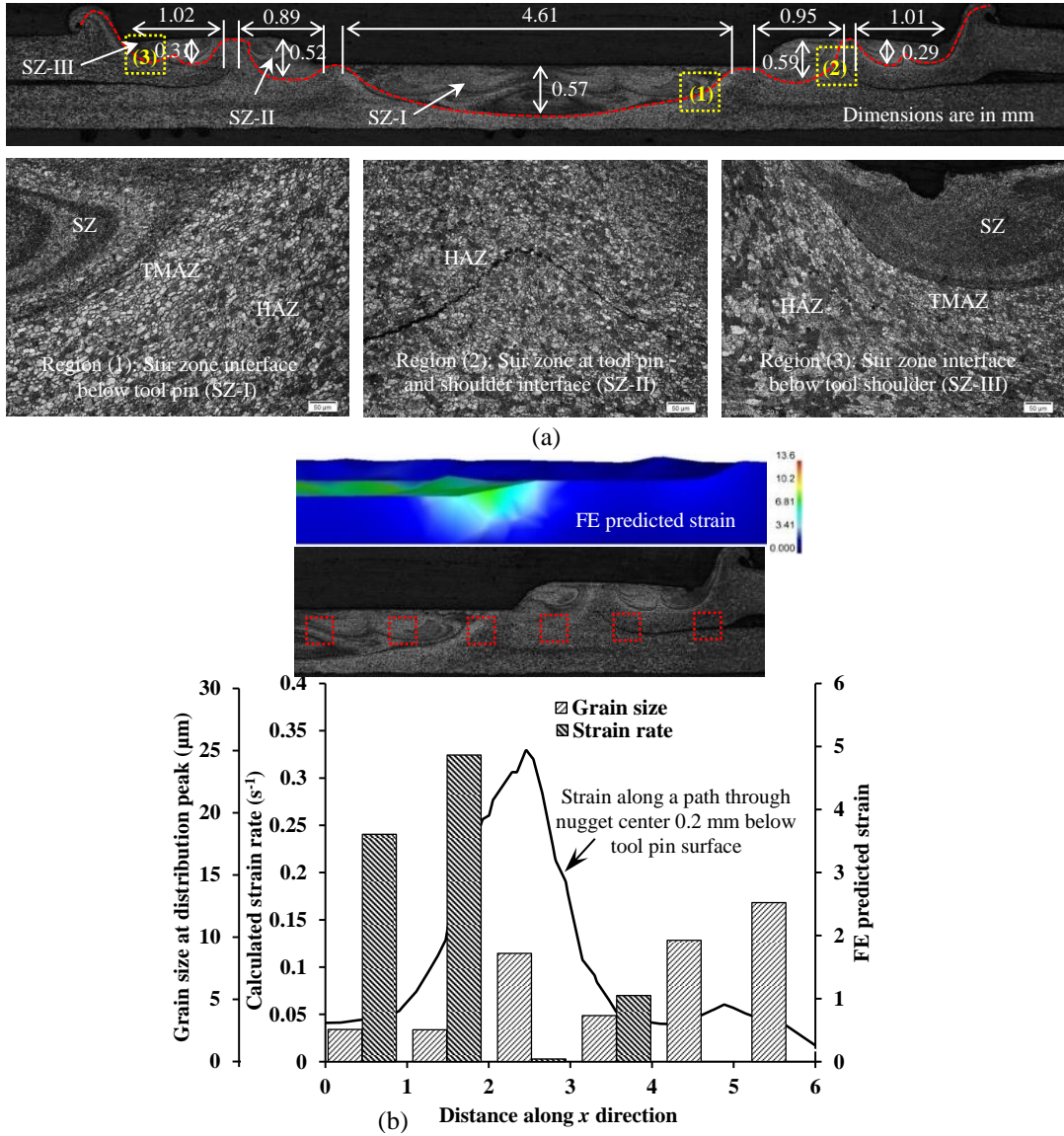


Figure 2. (a) Microscopic images of the weld cross-section and (b) variation of grain size distribution, strain, strain rate in FSSW joint made with circular pin ( $l = 0.2$  mm,  $h_p = 0.4$  mm)

Figure 2(b) shows the variation of measured grain size, FE predicted strain and calculated strain rate at different zones in and around the weld nugget region. The strain rate ( $\dot{\epsilon}$ ) during the FSSW process is calculated using the Zener-Hollomon relation given by:

$$Z = \dot{\epsilon} \exp\left(\frac{Q}{RT}\right) \quad (1)$$

where,  $T$  is the absolute temperature,  $R$  is universal gas constant and  $Q$  is the activation energy. In order to calculate the Zener-Hollomon parameter ( $Z$ ), the value of  $Q$  for AA6061 is taken as 156 kJ/mol (Gerlich et

al., 2007). Temperature ( $T$ ) is taken from the FE simulation results. The average temperature of the nodes in the different regions (along a path through the weld center and 0.2 mm below the tool pin) are considered when  $h_p = 0.4$  mm and for  $h_p = 0.6$  mm (circular tool pin), the path of measurement is 0.1 mm below the tool pin. For some of the aluminum alloys, the relationship between Zener-Hollomon parameter ( $Z$ ) and average recrystallized grain size ( $d$ , in  $\mu\text{m}$ ) is related as (Gerlich et al., 2007):

$$\log\left(\frac{d}{D}\right) = a_1 + b_1 \times \log(Z) \quad (2)$$

where  $a_1$  and  $b_1$  are material specific constants. For AA6061 these values are taken as  $a_1 = 1.75$  and  $b_1 = -0.244$  (Gerlich et al., 2007). The average grain size of the base material ( $D$ ) is measured as 20  $\mu\text{m}$ . The values of  $d$  at different zones are obtained considering sufficient number of grains. The grain size distributions in such zones are measured and grain size at the distribution peak is considered as the grain size ( $d$ ) of that zone for further calculation. The calculated value of  $Z$  for each such regions are obtained from Equation (2) and finally strain rate ( $\dot{\epsilon}$ ) is obtained from Equation (1). From Figure 2(b) it can be seen that in SZ-I significantly finer grain size is noticed ( $d$  at distribution peak 2.54 to 2.58  $\mu\text{m}$ ) as compared to base metal and the corresponding strain rate of 0.24 to 0.33  $\text{s}^{-1}$ . The FE predicted strain, calculated strain rate, and experimentally measured grain size indicate that the notable plastic deformation occurs in-and-around the tool pin periphery. It may be noted that the small change in the grain size produces the significant change in the calculated strain rate. It can also be observed from Figure 2(b) that away from the weld nugget (around 4.5 to 5.5 mm), the strain and strain rate decreases sharply and the grain refinement mainly occurred due to the welding heat. The grain size ( $d$ ) at distribution peak in these regions are noted in the order of 9.74  $\mu\text{m}$  and 12.77  $\mu\text{m}$  and strain rate calculated in the order of  $3 \times 10^{-4} \text{s}^{-1}$  and  $8.33 \times 10^{-6} \text{s}^{-1}$  (i.e.  $\approx 0$ , thus not visible in bar plot of Figure 2(b)).

Figure 3(a) shows the microscopic views of the interface of different zones formed below the tool for the FSSW joint prepared with circular tool pin with length  $l = 0.4$  mm ( $h_p = 0.6$  mm). Figure 3(a) indicates that with an increase in plunge depth the large volume of lower sheet material is pushed in the upward direction and the size of SZ-I formed below the tool pin is comparatively smaller for 0.6 mm plunge depth as compared to 0.4 mm plunge depth (refer Figure 2(a)). The width and depth of SZ-I are measured as 3.99 mm and 0.37 mm, respectively. As plunging progress the tool shoulder drags the large volume of plasticized material back towards the center of pin region and the large volume of material starts flowing in SZ-II region. Consequently, the size of the SZ-II increases due to stronger stirring and mixing action. The maximum width and depth of SZ-II are measured as 1.50 mm and 0.81 mm, respectively (Figure 3(a)) which is comparatively larger than that of circular tool pin with  $h_p = 0.4$  mm (maximum width and depth measured as 0.95 mm and 0.59 mm, respectively). Figure 2(a) and Figure 3(a) also indicates that the size of SZ-III is comparatively same in both the cases as the total shoulder penetration of 0.2 mm is constant. The maximum width of SZ-III for circular tool pin with 0.4 mm plunge depth is measured as 1.02 mm whereas for 0.6 mm plunge depth it is measured as 1.22 mm.

Figure 3(b) shows the variation of measured grain size, FE predicted strain and strain rate calculated using the Zener-Hollomon relationship at various zones of FSSW joint obtained with circular tool pin ( $h_p = 0.6$  mm). Figure 3(b) shows that with increase in plunge depth ( $h_p = 0.6$  mm) the calculated strain rate increased to 14  $\text{s}^{-1}$ . The increase in strain rate with increase in plunge depth could be due to the increase in contact area between the workpiece and tool surface thereby the thermal softening, easy flow and subsequent stirring of plasticized material due to the reduction in viscosity at the higher temperature. Therefore the large volume of plasticized material starts flowing around the tool pin periphery. From Figure 3(b) it can also be seen that the grain size (at distribution peak) in SZ-I for 0.6 mm plunge depth is measured around 3.29  $\mu\text{m}$  at maximum strain and strain rate below the tool pin region. Although a relatively lower strain and strain rate is observed near the SZ-II, a similar nature of fine size grains ( $d = 2.97 \mu\text{m}$  at distribution peak) are observed.

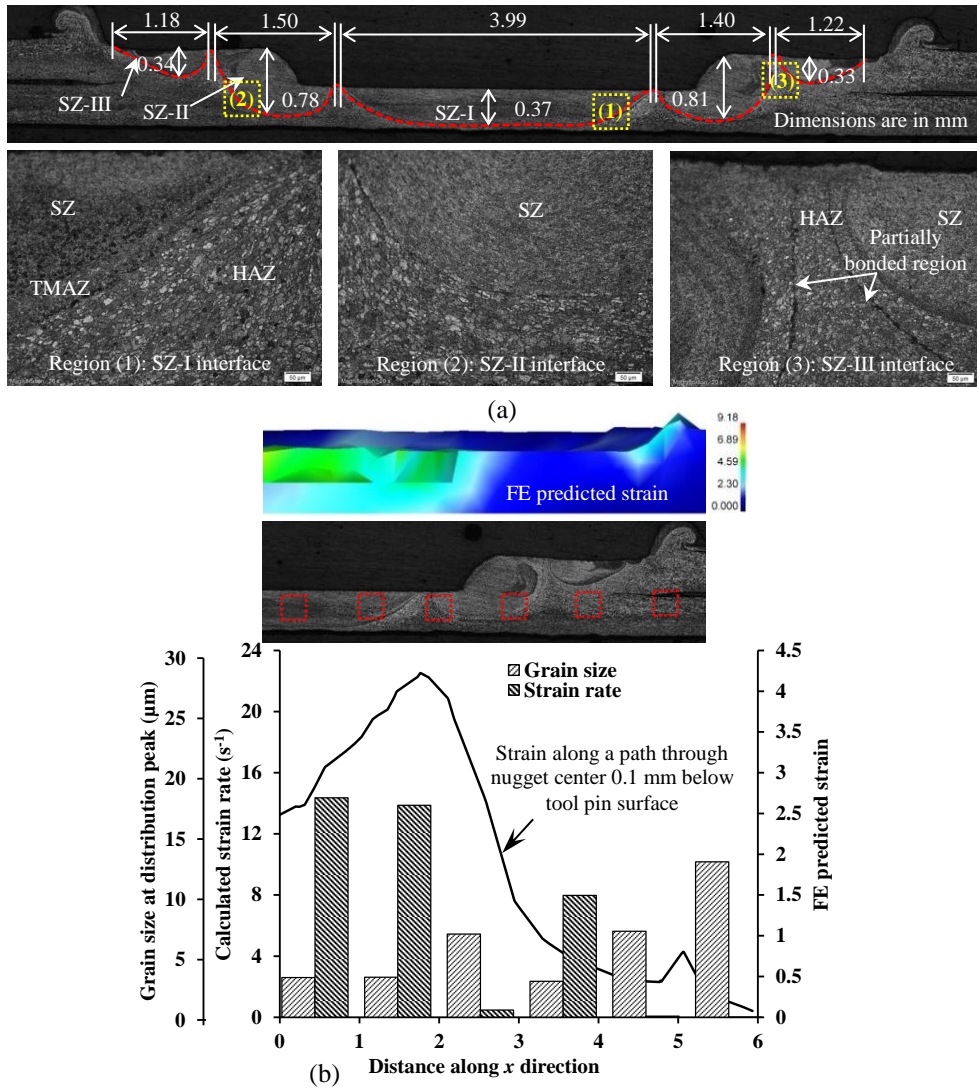
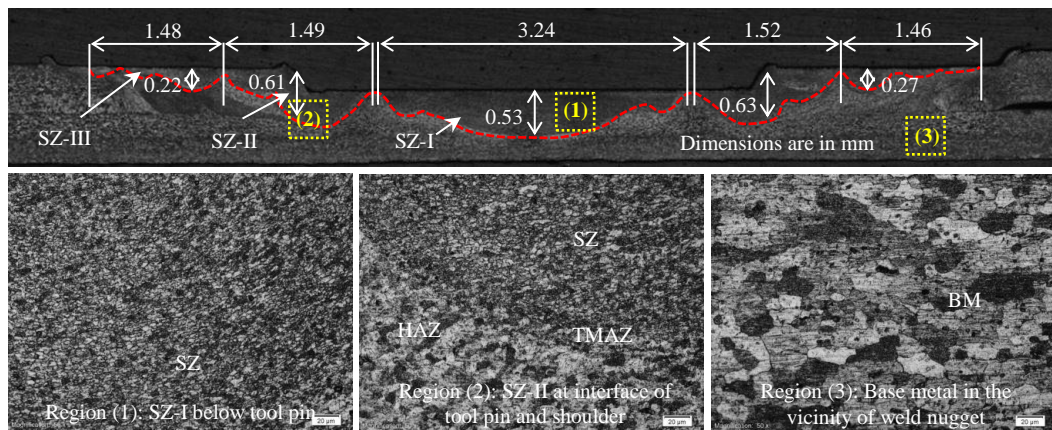


Figure 3. (a) Microscopic images of weld cross-section, (b) variation of grain size distribution, strain, strain rate in FSSW joint made with circular pin ( $l = 0.4$  mm,  $h_p = 0.6$  mm)

### Square Tool Pin

The microscopic images of the cross-section of weld prepared with square tool pin are shown in Figure 4(a). It may be noted that the size of SZ-I is comparatively smaller for square tool pin than circular tool pin for  $h_p = 0.4$  mm. The maximum width of SZ-I is measured as 3.24 mm and is little lesser than the case with circular tool pin for same plunge depth. The change in the size of the SZ with the change in the shape of tool pin can be attributed to the change in the swept volume rate (ratio of dynamic volume over static volume). It has been reported that the tool pin designed with the highest swept rate produces a stronger stirring and mixing action. Since the dynamic volume of circular and square is the same, it is the static volume that affects the swept rate (swept rate for the square pin 1.57). Also due to the higher swept rate for square tool pin profile and more material is accumulated around the tool pin periphery than the tool pin base thus the size of SZ-II formed at the interface of tool pin and shoulder is comparatively larger for square tool pin profile (maximum width and depth measured as 1.52 mm and 0.63 mm, respectively) as compared to circular tool pin profile (maximum width and depth measured as 0.95 and 0.59 mm, respectively) for same plunge depth of 0.4 mm (refer to Figure 2(a)).



(a)

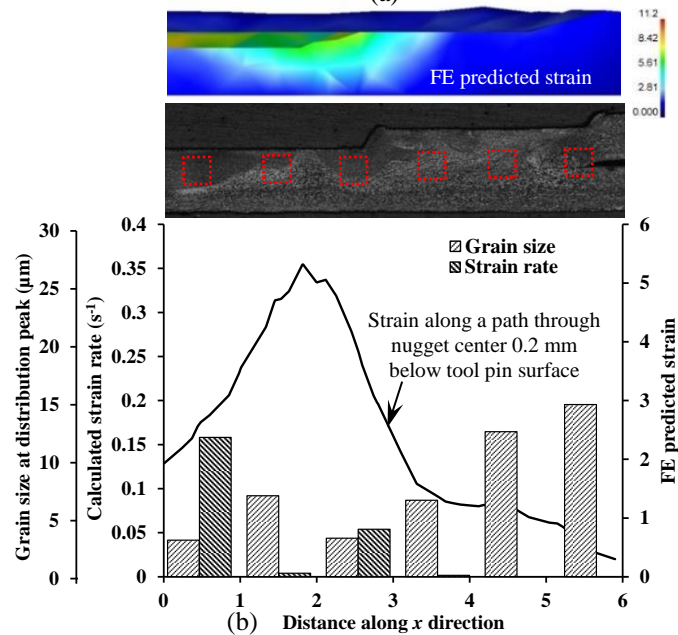


Figure 4. (a) Microscopic images of the weld cross-section, (b) variation of the grain size distribution, strain, strain rate in FSSW joint prepared with square pin ( $l = 0.2$  mm,  $h_p = 0.4$  mm)

Figure 4(b) shows the variation of measured grain size, FE predicted strain and calculated strain rate using the Zener-Hollomon expression for FSSW joint prepared with square tool pin ( $h_p = 0.4$  mm). From Figure 4(b) it can be observed that the calculated strain rate in SZ-I is about  $0.16 \text{ s}^{-1}$  and significantly finer grain size ( $d = 3.14 \text{ μm}$  at distribution peak) as compared to base metal is noted. Also for square tool pin (where swept rate is higher) slightly higher amount of strain (from FE results) is noted, but calculated strain rate is slightly lower than the circular tool pin. As stated earlier, a minor change in measured grain size can lead to a significant change in calculated strain rate. A similar magnitude of average grain size ( $3.31 \text{ μm}$  at distribution peak) is also observed in SZ-II region.

### Triangular Tool Pin

The microscopic views of cross-section of the welded joint prepared with triangular tool pin are shown in Figure 5(a). It may be noted from Figure 5(a) that the size of SZ-I (below tool pin surface) is comparatively smaller for triangular tool pin with maximum width and depth measured as 3.08 mm and

0.53 mm, respectively. The width of SZ-I below the tool pin for the triangular tool is noted comparatively smaller than the case with circular and square tool pin profile whereas the depth of SZ-I is observed to be similar for all tool pins with same plunge depth. Figure 5(a) shows that the size of SZ-II formed at the interface of tool pin and a tool shoulder of triangular tool pin have maximum width and depth 1.62 mm and 0.69 mm, respectively which is observed comparable to that of the square tool pin (maximum width and depth 1.52 mm and 0.63 mm, respectively) but higher than the case of circular tool pin (maximum width and depth measured as 0.95 and 0.59 mm, respectively). The change in the size of the SZ with the change in the shape of tool pin is mainly due to the change in the swept rate. The swept volume rate of 2.41 for triangular tool pin is quite higher than that for circular (swept rate of 1.0) and square tool pin (swept rate of 1.57), respectively. Thus more plasticized material is accumulated around the tool pin periphery than tool pin base and extended the size of SZ-II (around the interface of tool pin and shoulder) as compared to the size of SZ-I (below the tool pin surface).

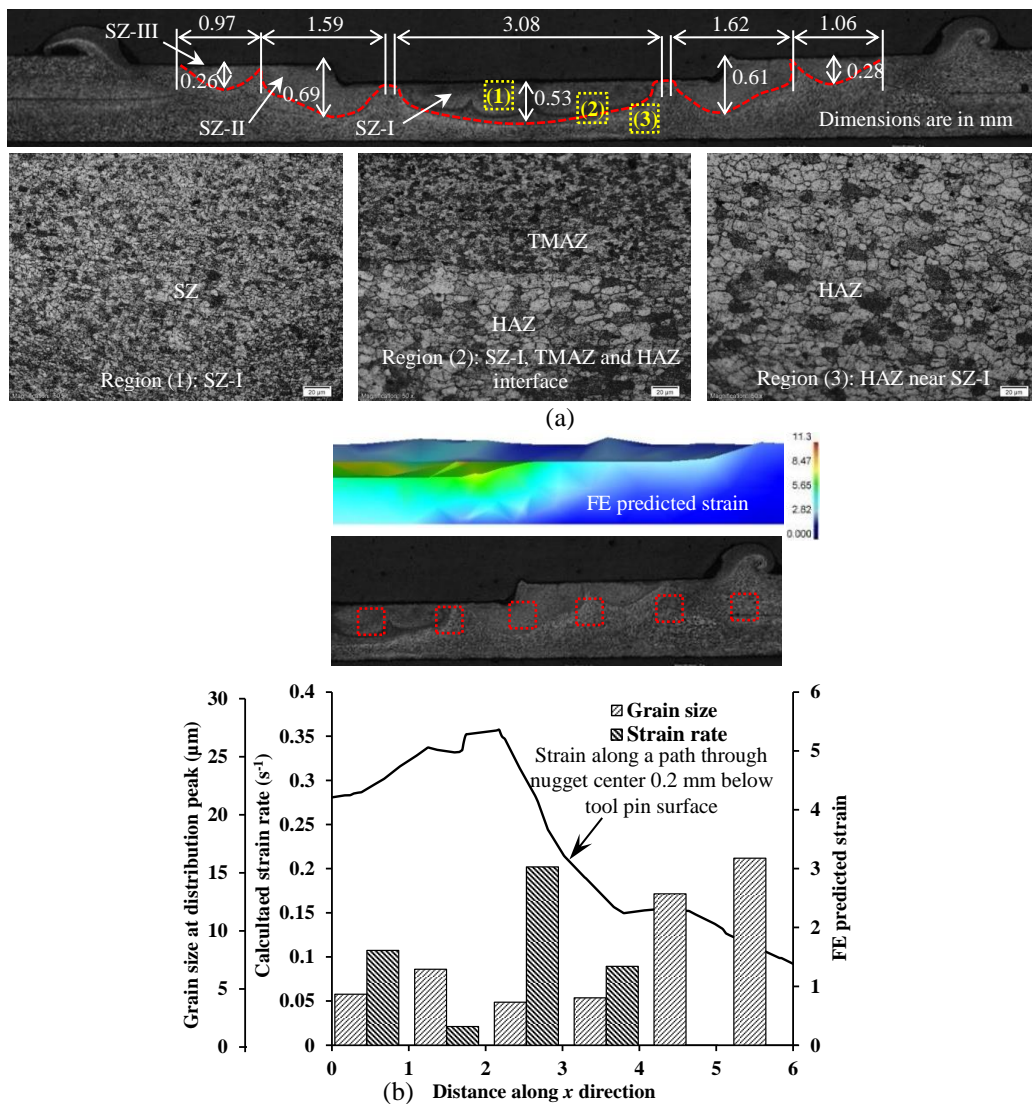


Figure 5. (a) Microscopic images of the weld cross-section and variation of (b) grain size distribution, strain, strain rate in FSSW joint made with triangular pin ( $l = 0.2$  mm,  $h_p = 0.4$  mm)

The variation of measured grain size, FE predicted strain and calculated strain rate at various zones of FSSW joint prepared with the triangular pin ( $h_p = 0.4$  mm) is represented in Figure 5(b). It may be easily noted that the calculated strain rate remains almost in the similar range when the tool pin shape changes from a square to triangular (refer Figure 4(b) and Figure 5(b)). From Figure 5(b) it can be seen that the smallest grain size of  $3.69 \mu\text{m}$  is obtained at the maximum strain rate of  $0.2 \text{ s}^{-1}$ .

For different tool pin profiles it may also be noticed that the average grain size within the stir zone lies in the range of  $2.54 \mu\text{m}$  to  $3.69 \mu\text{m}$  for same plunge depth. This marginal difference in grain size for different tool pins may be due to the small contact duration between the tool and workpiece in the FSSW process. However the size of the different zones in-and-around the weld nugget region formed with different tool pins are notably different.

### Micro-Hardness

Micro-indentation is performed on the welded specimens and the variation along the joint for different cases is shown in Figure 6. It may be observed from Figure 6 that the hardness of welded region is quite softened than the base metal hardness ( $112 \pm 2$  HV) which is mainly associated with a high friction and plastic deformation induced thermal cycle that softened the material. The variation of hardness is observed on either side of the weld center and higher hardness is observed at the intersection of SZ-II and TMAZ region. Towards the weld center hardness drops in the SZ-I region which undergoes intensive plastic deformation, highest heat generation thereby softens the material as compared to TMAZ region. Figure 6 also indicates that the hardness in SZ-I region is lower for the welded joint with 0.6 mm plunge depth (average hardness measured as 69 HV) than 0.4 mm plunge depth (average hardness measured as 73 HV). This might be because the heat generation for 0.6 mm plunge depth is higher than that of 0.4 mm plunge depth which considerably softens the material in SZ-I. For square tool pin ( $h_p = 0.4$  mm) the maximum hardness of 75 HV is obtained in SZ-II region which gradually decreases towards the weld center where the average hardness of about 70 HV is observed which is marginal lesser than that of circular tool pin. Figure 6 also shows that for triangular pin the maximum hardness (81 HV) is obtained in TMAZ region whereas the average hardness of about 67 HV is obtained in SZ-I region. For different tool pin profiles (with same plunge depth) the average hardness measured in the SZ-I region differs marginally (lies in range of  $70 \pm 3$  HV).

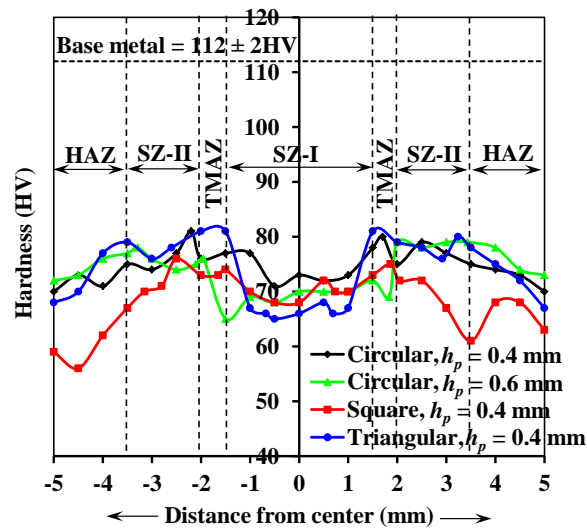


Figure 6. Micro-hardness variation plot in FSSW joints built by different tool pin profiles

## CONCLUSIONS

In the present work, the influence of different tool pin profiles and plunge depth on the formation of different stir zones, grain size distribution, strain, strain rate were studied and analyzed during FSSW of AA6061-T6. The results so obtained are summarized as follows:

- Microstructure observation revealed that the depth of the stir zone formed below the tool pin surface is almost similar with different tool pin profiles for same plunge depth ( $h_p = 0.4$  mm) but a wider stir zone is observed with circular tool pin.
- With increase in total plunge depth ( $h_p$ ) from 0.4 mm to 0.6 mm the size of the stir zone formed around the intersection of tool pin and shoulder increases for circular tool pin profile.
- For square and triangular tool pin (i.e. with higher swept volume rate) due to the stronger stirring and intermixing, comparatively larger stir zone is observed at the tool pin and shoulder intersection region.
- Grain size measurement indicates the formation of finer equiaxed grains in stir zone as compared to other zones due to the continuous dynamic recrystallization of grain structure.
- Grain size measurement also indicates that the average grain size measured in stir zone for different tool pin profiles is comparable but significantly finer than the grain structure of base metal.
- Micro-hardness measurement indicates that the welded region is quite softened than the base metal and maximum hardness among various zones is observed mostly around the thermo-mechanically affected zone.

## REFERENCES

- Chang, C.I., Lee, C.J., & Huang, J.C. (2004). Relationship between grain size and Zener–Holloman parameter during friction stir processing in AZ31 Mg alloys. *Scripta Materialia*, 51, 509–514.
- Fratini, L., & Buffa, G. (2005). CDRX modelling in friction stir welding of aluminium alloys. *International Journal of Machine Tools and Manufacture*, 45, 1188–1194.
- Garg, A., & Bhattacharya, A. (2017a). On lap shear strength of friction stir spot welded AA6061 alloy. *Journal of Manufacturing Processes*, 26, 203–215.
- Garg, A., & Bhattacharya, A. (2017b). Strength and failure analysis of similar and dissimilar friction stir spot welds: Influence of different tools and pin geometries. *Materials & Design*, 127, 272–286.
- Gerlich, A., Yamamoto, M., & North, T.H. (2007). Strain rate and grain growth in Al 5754 and Al 6061 friction stir spot welds. *Metallurgical and Materials Transactions A*, 38, 1291–1302.
- Gerlich, A., Yamamoto, M., & North, T.H. (2008). Local melting and tool slippage during friction stir spot welding of Al-alloys. *Journal of Materials Science*, 43, 2–11.
- Hirasawa, S., Badarinarayan, H., Okamoto, K., Tomimura, T., & Kawanami, T. (2010). Analysis of effect of tool geometry on plastic flow during friction stir spot welding using particle method. *Journal of Materials Processing Technology*, 210, 1455–1463.
- Reilly, A., Shercliff, H., Chen, Y., & Prangnell, P., (2015). Modelling and visualisation of material flow in friction stir spot welding. *Journal of Materials Processing Technology*, 225, 473–484.
- Sarkar, R., Pal, T.K., & Shome, M. (2016). Material flow and intermixing during friction stir spot welding of steel. *Journal of Materials Processing Technology*, 227, 96–109.
- Solhjo, S. (2010). Determination of critical strain for initiation of dynamic recrystallization. *Materials & Design*, 31, 1360–1364.